Change of tropical cyclone activity by Pacific-Japan teleconnection pattern in the western North Pacific

Ki-Seon Choi,[1] Chun-Chieh Wu,[1] and Eun-Jeong Cha[2]

Received 14 January 2010; revised 10 March 2010; accepted 22 April 2010; published 9 October 2010.

[1] This study shows that the Pacific-Japan (PJ) teleconnection pattern has a significant influence on tropical cyclone (TC) activities over the western North Pacific (WNP) during the boreal summer (July, August, and September). During positive (negative) PJ phase, TCs form at a more northward (southward) location, recurve at a more northeastward (southwestward) location, and frequently pass over the northeast Asian (southeast Asian) region, including Korea and Japan (South China Sea and southern China). In particular, this difference in the TC track between the two phases is observed as a dipole-like pattern between the regions of Southeast and Northeast Asia. The TC characteristics during the positive PJ phase are caused by the following two stronger atmospheric circulations over the WNP: an anticyclonic circulation centered to the east of Japan and a cyclonic circulation centered to the east of Taiwan. The southeasterly between these two circulations serves as steering flow that TCs move northward toward Korea and Japan from the northeast of the Philippines. Conversely, TCs during the negative PJ phase mainly move westward toward the South China Sea and southern China by the easterly from a stronger anticyclonic circulation centered to the east of Taiwan. As a result of this feature of TC track during the negative PJ phase, TC lifetime is shorter and TC intensity is weaker.

Citation: Choi, K.-S., C.-C. Wu, and E.-J. Cha (2010), Change of tropical cyclone activity by Pacific-Japan teleconnection pattern in the western North Pacific, *J. Geophys. Res.*, *115*, D19114, doi:10.1029/2010JD013866.

1. Introduction

[2] The various East Asian summer climates, including tropical cyclone and summer monsoon rainfall, are the main issue in East Asian community, because they have significant impact on the living and economy of people in East Asia including farming and natural disasters. These meteorological phenomena are controlled by various large-scale circulations: a combination of the western North Pacific (WNP) high (WNPH), the upper-level Tibetan high, the Okhotsk high, and the monsoon trough in the low-latitudes prevailing during the boreal summer. These large-scale atmospheric circulations can be represented by the Pacific-Japan teleconnection pattern (hereafter, PJ pattern), which is one of dominant atmospheric anomaly patterns that influence East Asian summer climate conditions. The PJ pattern is characterized by anomalous circulation between the subtropics and midlatitudes over the WNP in the lower troposphere, which is a meridional dipole of anomalous circulation between two regions [*Nitta*, 1986, 1987, 1989]. *Nitta* [1987, 1989] pointed out that PJ pattern is closely related to SST distribution in the warm pool region and can be understood as the forced mode generated by SST forcing (external forcing), not the free mode existing in an atmosphere which is the internal mode or dynamic mode. However, *Nitta*'s [1986, 1987, 1989] analysis is based on data only for a 6-year period of 1978 to 1983, and thus his result may not be substantial enough for obtaining robust statistics. Since the pioneering work of *Nitta* [1987, 1989], many PJ pattern studies have been carried out to investigate its relevant impact on summer climate, particularly on the East Asian summer monsoon [*Huang and Li*, 1987; *Kurihara and Tsuyuki*, 1987; *Murakami and Matsumoto*, 1994]. *Tsuyuki and Kurihara* [1989] showed that the intraseasonal PJ pattern tends to be more significant in midsummer than in early summer rainy season. *Kawamura et al.* [1996] revealed that the lower-level southwesterly jet is associated with summer monsoon southwesterly serves as a waveguide of PJ pattern and that such a waveguide with the PJ pattern disappears in autumn because the summer monsoon southwesterly retreats due to the cooling of the Asian continent. *Kawamura et al.* [1998] showed that anomalous SST forcing from the tropics is responsible for frequent occurrence of extraordinary summers in Japan after the late 1970s by performing an ensemble of climate experiments. In particular, they demonstrated more concretely results of *Nitta* [1987, 1989] that PJ pattern is force mode through this ensemble. However, *Kosaka and Nakamura* [2006] suggested that the PJ pattern also can be inter-

[1]Department of Atmospheric Sciences, National Taiwan University, Taipei, Taiwan.
[2]National Typhoon Center, Korea Meteorological Administration, Jeju, South Korea.

0148-0227/10/2010JD013866

preted as a dynamical mode in the atmosphere inherent to the boundary region between the continental Asian summer monsoon to the west and the WNPH to the east. As stated above, most researches related to the PJ pattern focus mainly on changes of East Asian summer monsoon. However, the TC activity also plays a significant role in the variation of East Asian summer climate and, in particular, is the potential factor that may have significant impact on rainfall in a short-range period. The TC may be also influenced by large-scale circulation from PJ pattern, and thus this study analyzes a relationship between PJ pattern and TC activity in the western North Pacific.

[3] Studies on the association between the TC and PJ pattern are not found as much as studies on the relationship between the PJ pattern and the East Asian summer monsoon. Most of the former studies focus on how large-scale disturbances such as TCs trigger a wave train to the east of the Philippines (warm pool region). In other words, these studies are more interested in the changes of the PJ pattern by TC activity. However, it is not yet clear whether TCs over the warm pool region of a WNP could also trigger a similar extratropical wave train. More recently, *Kawamura and Ogasawara* [2006] showed that TCs which are synoptic-scale convective heating sources over the subtropical WNP can induce the barotropic Rossby wave train and consequently influence anomalous summer climate around Japan through a remote forcing. They also pointed out that the zonal pressure gradient at lower levels between a TC and a PJ-induced anomalous anticyclone to the east of Japan reinforces warm advection and moisture supply from the low-latitudes. As a result, a TC triggers heavy rainfall along the Pacific coast of the mainland Japan, despite the long distance in between them. Their results exhibit a dynamical relationship between the TC activity and the PJ pattern, but their analysis is confined in only one month (in August). *Yamada and Kawamura* [2007] set up the hypothesis that the TC activity over the WNP is high in autumn as well as in summer, and the TCs are expected to occur and develop in higher latitudes, which might increase the occurrence of extratropical wave trains due to the TCs. Then they demonstrated that the relationship between the PJ pattern and the TC activity contributes significantly to activities of the summer rainy front (Baiu front) in early summer and/or the autumn rainy front (Akisame front). However, as the priority of the two variables (TC and PJ pattern) and the three dimensional structure of the PJ pattern have not been fully analyzed, a question on how TC activities trigger wave trains is also open to debate.

[4] The present study focuses on the examination of the change of WNP TC activity by the PJ pattern. This may be because the result of the current study can be helpful in future studies on the seasonal prediction of TC activities, if the PJ pattern is predictable before the summer season (TC season).

[5] The data and analysis methods used in this study are described in section 2. In section 3, the PJ pattern is defined and positive PJ and negative PJ years are also selected. The correspondence between WNP TC activity (e.g., the genesis, passage, recurvature, intensity of TCs and their relations with large-scale environments such as atmospheric circulation and sea surface temperature) and the variation of PJ pattern is investigated in section 4. Finally, section 5 summarizes the paper.

2. Data and Methodology

2.1. Data

[6] The information about TC activity is obtained from the best track archives of the Regional Specialized Meteorological Center (RSMC), Tokyo Typhoon Center. The data sets consist of TC names, longitude and latitude positions, minimum surface central pressures, and maximum sustained wind speeds (10-min average maximum winds to the nearest 5 kts) measured every 6 h from 1965 to 2008 (44 years). TCs are generally divided into four categories based on their maximum sustained wind speed (MSWS): tropical depression (TD, MSWS < 34kts), tropical storm (TS, 34kts ≤ MSWS ≤ 47kts), severe tropical storm (STS, 48kts ≤ MSWS ≤ 63kts), and typhoon (TY, MSWS ≥ 64kts). The present study focuses on extratropical cyclones (ETs) that transformed extratropically from TCs as well as TCs of four categories. ETs are included in the analysis because they cause damages in the midlatitudes of East Asia.

[7] We also use the geopotential height (gpm), horizontal wind (m s^{-1}), and vertical velocity (hPa s^{-1}) data sets reanalyzed by the National Centers for Environmental Prediction-National Center for Atmospheric Research (NCEP-NCAR) [*Kalnay et al.*, 1996; *Kistler et al.*, 2001]. These NCEP-NCAR reanalysis data sets have a horizontal resolution of 2.5° × 2.5° latitude-longitude and are available for the period of 1948 to the present. Also, NOAA interpolated Outgoing Longwave Radiation (OLR) data, retrieved from the NOAA satellite series, are available from June 1974 to present in NOAA's Climate Diagnosis Center (CDC). However, the data includes a missing period from March to December of 1978. More detailed information about OLR data can be found on the CDC website (http://www.cdc.noaa.gov) or in the paper by *Liebmann and Smith* [1996]. The NOAA Extended Reconstructured monthly Sea Surface Temperature (SST) [*Reynolds et al.*, 2002], available from the same organization, is also used. The data have a horizontal resolution of 2.0° × 2.0° latitude-longitude and are available for the period of 1854 to the present.

[8] While TC data are accessible for the period from 1951 to the present, the reliability of TC data in the 1950s and early 1960s prior to the weather satellite era could lead to problems [*Ho et al.*, 2005]. The NCEP-NCAR reanalysis data are also affected by two major changes in the observing system, upper air networks and satellite observations [*Kistler et al.*, 2001]. To avoid any possible impact of unreliable data on the present results, all calculations are confined to the period from 1965 to 2008, during which weather satellites are used.

2.2. Methodology

[9] To calculate the TC passage frequency (TCPF), each TC position is binned into a corresponding 5° × 5° grid box, and a TC is only counted once even though it may enter the same grid box several times [*Ho et al.*, 2005]. The TC genesis frequency (TCGF) is calculated by the same method for TCPF. About 60% of the annual number of TCs occur in July, August, and September (JAS) over the WNP [e.g., *Chia and Ropelewski*, 2002]. Therefore, the present study

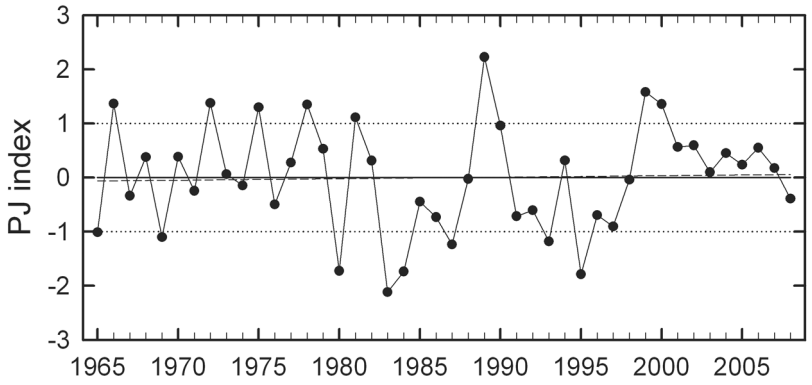

Figure 1. Time series of the normalized index of the Pacific-Japan (PJ) teleconnection pattern during the summer (July, August, and September (JAS)). Dashed line denotes a trend.

uses 3-month data sets and these months are defined as the boreal summer.

[10] For the significance test in this study, the statistical method of Student's *t* test is used [e.g., *Wilks*, 1995]. In case that two independent time series follow a *t* distribution and their time averages are denoted as $\bar{x}_1$ and $\bar{x}_2$ respectively, the test statistic is given by

$$t = \frac{\bar{x}_1 - \bar{x}_2}{\left(s_1^2/n_1 + s_2^2/n_2\right)^{1/2}}$$

where, S_1 and S_2 are standard deviations, and n_1 and n_2 are numbers of the two time series, respectively. From the above formula, if the absolute value of t is greater than threshold values with a level of significance, the null hypothesis would be rejected at the α ($\times$ 100)% significance level.

3. Definition of Pacific-Japan (PJ) Index

[11] *Wakabayashi and Kawamura* [2004] applied an empirical orthogonal function (EOF) analysis to the 850 hPa monthly stream function anomaly fields that computed from the NCEP-NCAR reanalysis data, and then they defined the PJ pattern as the difference in 850-hPa geopotential height anomalies between two grid points (155°E, 35°N: region east of Japan and 125°E, 22.5°N: region east of Taiwan) in the dominant stream function anomaly pattern during the boreal summer. *Kawamura and Ogasawara* [2006] and *Yamada and Kawamura* [2007] calculated using the definition of *Wakabayashi and Kawamura* [2004] a period exceeding +1.5σ as an event in which the PJ pattern predominates from the north of the Philippines through the central North Pacific.

[12] In the present study, the PJ index (PJI) is calculated by using the definition of *Wakabayashi and Kawamura* [2004] as shown in the formula below

$$PJI = Z_{850}(35^\circ N, 155^\circ E) - Z_{850}(22.5^\circ N, 125^\circ E)$$

where, Z_{850} represents the geopotential height at the 850 hPa level.

[13] Climatologically, a monsoon trough in the southeast of Taiwan and a WNPH in the east of Japan are distinctive during the boreal summer. This monsoon trough extends to the region east of the WNP, and thus it makes a preferred region for TC genesis [*McBride*, 1995]. The WNPH extends northwestward, and thus it plays a critical role in determining TC movement toward the midlatitudes of East Asia. Therefore, the PJI can be used in determining not only the intensity between these two pressure systems but also WNP TC activity.

[14] Figure 1 shows a normalized summer PJI using the above definition for 44 years. Here, climatological summer mean value is defined as one averaged for 44 years. This trend of PJI time series is nearly constant for 44 years (0.02 yr^{-1}). In order to examine characteristics of the change of the WNP TC activity by the PJ pattern, the highest 8 positive PJ years and the lowest 8 negative PJ years, respectively are selected from the normalized PJI time series (Table 1). These years all have standardized values higher (less) than +1 (−1). However, the PJI time series has a weak negative relation (r = −0.19) with Niño-3.4 index in JAS during the entire analysis period (not shown). Although this result is not statistically significant, it cannot be assured that results in this study are fully independent of El Niño/Southern Oscillation (ENSO) effects. Thus, this study newly defines the highest 8 positive and the lowest 8 negative PJ years only from neutral ENSO years (i.e., excluding El Niño and La Niña years) to compare with characteristics of PJ phases with ENSO years (Table 1). Here, El Niño and La Niña years are defined when the threshold (El Niño: +0.5°C, La Niña: −0.5°C) of 3 month running mean of SST anomalies in the Niño-3.4 region (5°N–

Table 1. Eight Positive PJ Years and Eight Negative PJ Years With ENSO Years and Selected From Neutral ENSO Years in the Time Series of Figure 1[a]

PJ Phase	ENSO Effects	Years
Positive	Included	1966 **1972** *1975* 1978 1981 1989 *1999* 2000
	Excluded	1966 1979 1990 1978 1981 1989 2001 2000
Negative	Included	**1965** 1969 1980 1983 1984 **1987** 1993 1995
	Excluded	1976 1969 1980 1983 1984 1992 1993 1995

[a]Boldface and italics denote El Niño and La Niña years, respectively.

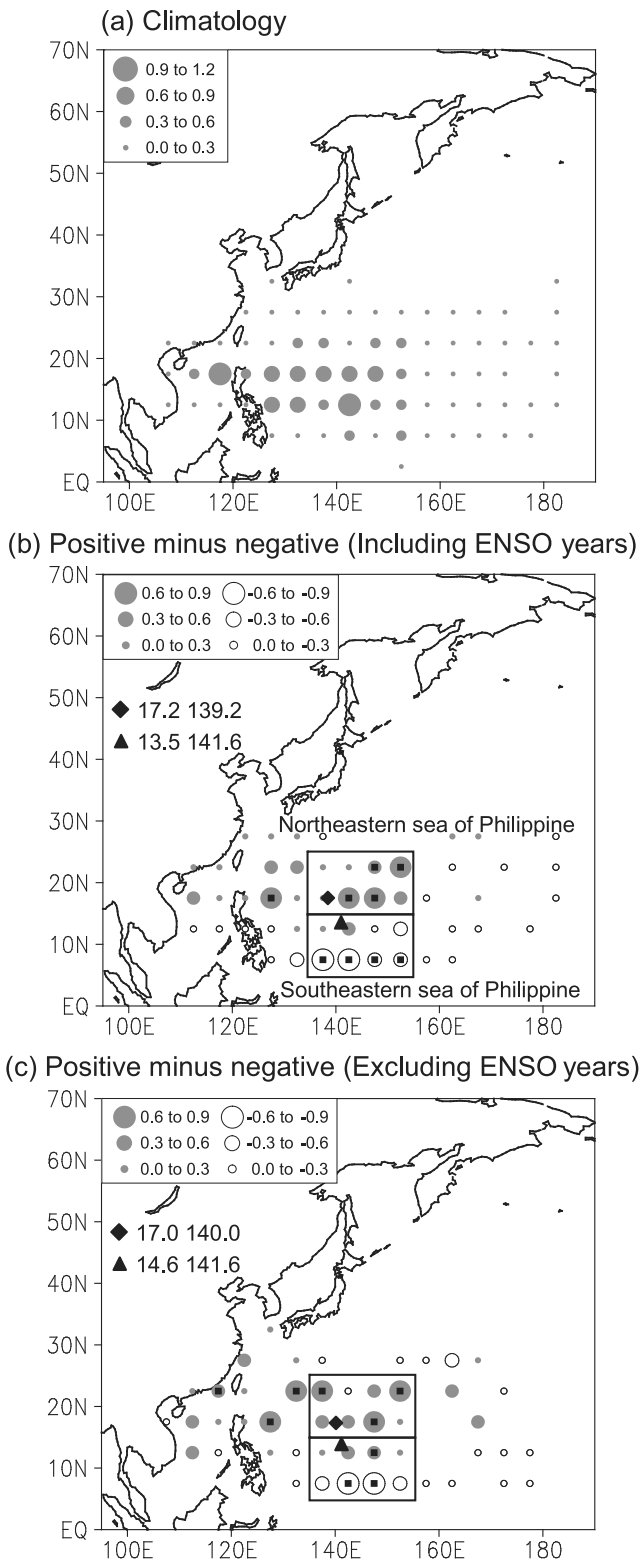

Figure 2. (a) Summer (JAS) tropical cyclone (TC) genesis frequency (TCGF) for climatology, and differences in TCGF between the positive and negative PJ phases (b) with ENSO years and (c) selected from neutral ENSO years. Diamond and triangle denote mean genesis locations of the positive and negative PJ phases, respectively. Small squares within circles are significant at the 95% confidence level.

5°S, 170°W–120°W) is met for a minimum of 5 consecutive over-lapping seasons (http://www.cpc.noaa.gov/products/analysismonitoring/ensostuff/ensoyears.shtml).

4. Characteristics of TC Activity by the PJ Pattern

[15] In this section, we analyze differences in TC activities (TCGF, TCPF, TC recurvature, and TC intensity) and large-scale environments (atmospheric circulation and SST) between positive and negative PJ phases.

4.1. TC Genesis Frequency

[16] Figure 2 shows the spatial distributions of the climatology and the difference between positive and negative PJ phases on the TC genesis frequency (TCGF) over the WNP within each 5° × 5° latitude-longitude grid box. Climatological values of the TCGF are defined by dividing the total genesis frequency of TCs during the boreal summer by 44 (44 years). Also, the differences between positive and negative PJ phases are defined as the subtraction of the average in eight negative PJ years from the average in eight positive PJ years.

[17] Many TCs occur around the Philippine Sea where SSTs are high, which is generally referred to as the warm pool region in the tropical WNP (Figure 2a). The center of TC genesis is located in the SCS and the sea east of the Philippines.

[18] On the other hand, total TCGFs in each positive PJ phase and negative PJ phase with ENSO years are 140 (average: 17.5 TCs) and 108 (average: 13.5 TCs), respectively (Table 2). This implies that on average, the number of TCs occurring in each summer during the positive PJ phase exceeds that in the negative PJ phase by four. The mean genesis location is 17.2°N, 139.2°E for the positive PJ phase and 13.5°N, 141.6°E for the negative PJ pattern, which indicates that TCs in the positive PJ phase tend to occur more toward the northwest than those in the negative PJ phase (Table 2). In the monthly TCGF in each phase, 44, 50, and 46 TCs occurred in July, August, and September during the positive PJ phase and 31, 40, and 37 TCs during the negative PJ phase. In particular, the differences in each monthly TCGF between the two PJ phases are 12, 11, and 9 TCs in July, August, and September, and thus their differences are not concentrated in any one month. Therefore, the summer mean variables are used in the following analyses.

[19] These features are also observed in differences in TCGF (27 TCs), TC genesis location (2.4°N, −1.6°E,) and monthly TCGF (8 TCs, 11 TCs, and 8 TCs) between the two PJ phases that are selected from neutral ENSO years (Table 2).

[20] On the other hand, with regard to the difference in the TCGF between the positive and negative PJ phases with ENSO years (Figure 2b), over the region west of 155°E, more TCs occur in the region north (south) of 15°N during the positive (negative) PJ phase. In particular, a relatively large difference in the TCGF between the two PJ phases is shown to the east of the Philippines (5°–25°N, 135°–155°E). *Ho et al.* [2005] demonstrated that a large difference in the TCGF between the positive Antarctic Oscillation (AAO) and negative AAO phases is distinctive in this region. *Choi and Byun* [2010] also pointed out that more TCs

Table 2. Statistics on Average TC Activity for the Highest Eight Positive and the Lowest Eight PJ Years With ENSO Years and Selected From Neutral ENSO Years[a]

TC Activity	Including ENSO Effects PJ Phase		Excluding ENSO Effects PJ Phase	
	Positive	Negative	Positive	Negative
Annual genesis frequency	**17.5**	**13.5**	**16.5**	**13.2**
Genesis location				
Latitude (°N)	**17.2**	**13.5**	**17.0**	**14.6**
Longitude (°E)	139.2	141.6	140.0	141.6
Recurvature location				
Latitude (°N)	29.6	27.8	30.1	27.3
Longitude (°E)	**136.6**	**128.7**	**136.4**	**130.4**
Intensity				
CP at recurvature (hPa)	974.1	983.9	976.9	984.9
Lifetime (day)	**11.2**	**8.0**	**10.8**	**8.3**
Min CP during the lifetime (hPa)	**958.8**	**969.5**	**963.4**	**971.5**

[a]The abbreviation CP represents the TC central pressure. Bold numbers denote that the difference between the two PJ phases in each TC activity is significant at the 99% confidence level and at the 95% confidence level for the remaining numbers.

during the positive Arctic Oscillation (AO) phase tend to occur in this region. Afterwards, this study refers to the sea northeast of the Philippines as Northeastern sea of Philippine (15°–25°N, 135°–155°E) and the sea southeast of the Philippines as Southeastern sea of Philippine (5°–15°N, 135°–155°E), and a difference in the TCGF between the two PJ phases is examined in these two regions (Figure 3). Climatologically, 7.0 TCs occur in the summer of each year with a standard deviation of 3.1 TCs in the Northeastern sea of Philippine. During the positive PJ phase, the TCGF is lower than climatological mean value only for two years (1999 and 2000). On the contrary, the TCGF during the negative PJ phase is higher than the climatological mean value for only two years (1965 and 1980) (Figure 3a). In particular, approximately 3 more TCs occur during the positive PJ phase than during the negative PJ phase. This difference is significant at the 95% confidence level. On the other hand, 3.7 TCs climatologically occur in the summer of each year with a standard deviation of 2.3 TCs in the Southeastern sea of Philippine, which is equivalent to about half of the climatological mean value in the Northeastern sea of Philippine (Figure 3b). The TCGF during the positive PJ phase is higher than the climatological mean value only for three years (1966, 1972, and 2000). The climatological mean value, in particular, is lower than the figure in the negative PJ phase by 2 TCs, which is significantly at the 90% confidence level. This regional difference in a TCGF over the WNP is also found in the difference between the two PJ phases that are selected from neutral ENSO years (Figure 2c), In addition, differences in the TCGF averaged in two areas over the WNP between these two PJ phases are observed as well (not shown): 2.4 TCs (positive: 8.1, negative: 5.7) for Northeastern sea of Philippine and −1.1 TCs (positive: 3.6, negative: 4.7) for Southeastern sea of Philippine. However, only the former difference is significant at the 90% confidence level.

4.2. TC Passage Frequency

[21] Figure 4 shows the spatial distributions of climatology and the differences between the positive and negative PJ phases in relation with TC passage frequency (TCPF) during the boreal summer within each 5° × 5° latitude-longitude grid box. Climatological values and the TCPF differences between the two PJ phases are calculated using the same method used for the TCGF. Since TCs generally tend to migrate along the western periphery of the WNPH, the TCPF is higher over the South China Sea and the East China Sea (Figure 4a). Over the two regions, more than 2.0 TCs are shown in each 5° × 5° grid box every boreal summer. The TCPF also indicates the passage track (areas with more than 1.5 TCs) elongated toward Korea and Japan.

[22] The difference in a TCPF between the two PJ phases with ENSO years are clearly distinguishable (Figure 4b). During the positive PJ phase, TCs tend to migrate from the northeast of the Philippines, passing through the East China Sea, to Korea and Japan. However, TCs during the negative PJ phase mainly move from the southeast of the Philippines, passing through the Philippines and South China Sea, and

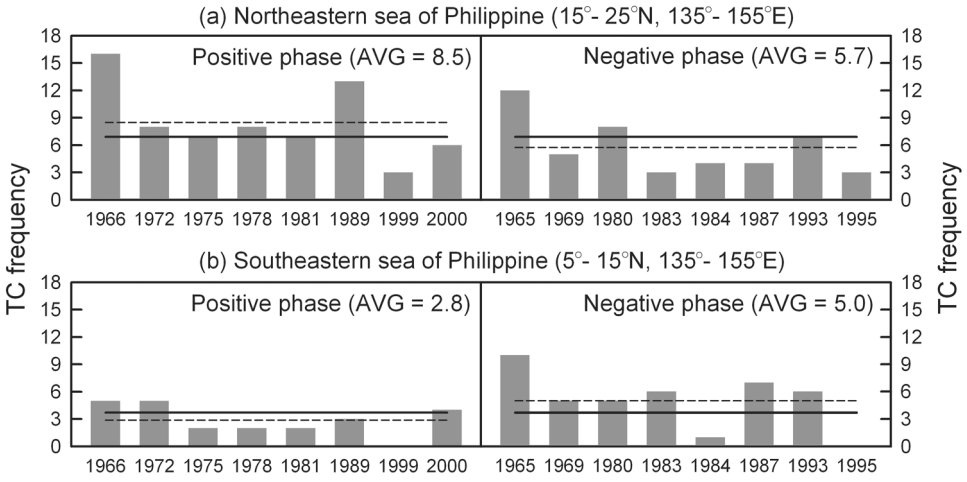

Figure 3. Summer (JAS) TCGF for two PJ phases with ENSO years in each area defined in Figure 2b. Dashed line denotes average for each PJ phase in each area. Thick solid line is a climatological mean TCGF in each area (Northern area: 6.9, Southern area: 3.7). AVG is abbreviation for average.

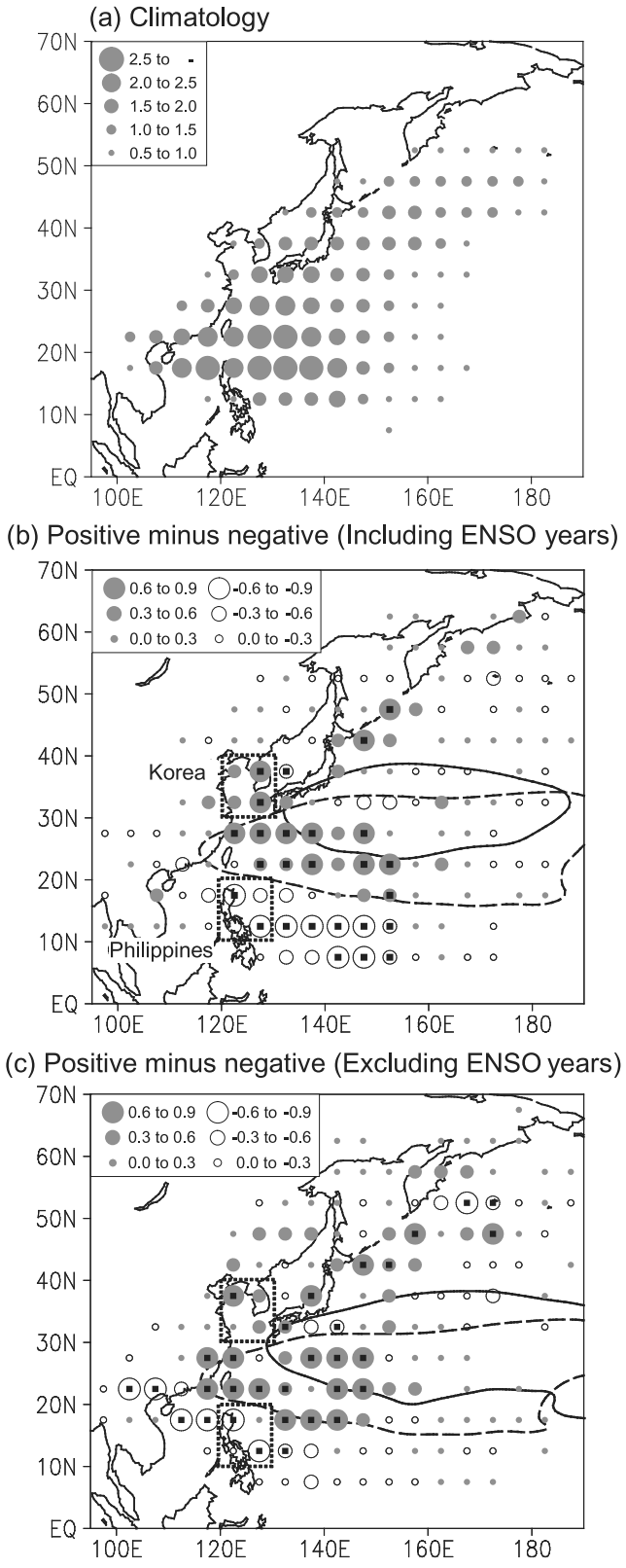

Figure 4. Same as in Figure 2 but for TC passage frequency (TCPF) for JAS. Solid and dashed contours indicate 5870 gpm for the positive and negative PJ phases, respectively.

finally land in southern China. In other wards, this spatial distribution shows a dipole-like pattern between the regions of Southeast and Northeast Asia. Eventually, it indicates that the passage of TCs during the positive PJ phase is located more toward the north than those during the negative PJ phase, which is similar to the result of the difference in a TCGF between the two PJ phases.

[23] From the dipole-like pattern in a TCPF, it is found that the countries in which the TCPF is relatively high during the positive and negative PJ phases are Korea (30°–40°N, 120°–130°E) and the Philippines (10°–20°N, 120°–130°E), respectively. Therefore, TCPFs for the two PJ phases are examined in each region (Figure 5). Korea is climatologically affected by 3.3 TCs with a standard deviation of 1.6 TCs during the summer of each year. The TCPF in the positive PJ phase not only is higher than the climatological mean value but also has approximately 1.5 more TCs than in the negative PJ phase. This difference between the two PJ phases is significant at the 90% confidence level. On the other hand, TCPF around the Philippines shows opposite characteristics comparing to Korea for both phases. In particular, it is found that there are no years that have TCPF higher than the climatological mean value (4.8 TCs with a standard deviation of 1.7 TCs) during the positive PJ phase. These features are also shown in the difference between the two PJ phases that are selected from neutral ENSO years (Figure 4c), However, differences in the TCPF averaged for two areas between the two PJ phases are not as large as differences between the two PJ phases with ENSO years: 1.0 TC (positive: 3.7, negative: 2.7) for Korea and −1.7 TCs (positive: 3.8, negative: 5.5) for Philippines. However, only the latter difference is significant at the 90% confidence level. Consequently, the difference in the TCPF between the two PJ phases in both Korea and the Philippines has a feature similar to that in the TCGF between the two PJ phases in two sea areas.

4.3. TC Recurvature

[24] Figure 6 shows the TC recurvature locations during the summer of the positive (black dots) and negative PJ (red dots) phases. Here, TC recurvature is defined as the point at which a TC turns northeastward from its northwestward movement, and thus non-recurved TCs are excluded in the analysis. In the case of two PJ phases with ENSO years (Figure 6a), 73 (about 52%) of the 140 TCs recurved during the positive PJ phase and 44 (about 41%) of the 108 TCs during the negative PJ pattern. This result demonstrates that more TCs during the negative PJ phase tend to move westward instead of going north toward the midlatitudes of East Asia, as indicated in Figure 4b. In addition, it is shown that there is a pronounced difference in the TC recurvature locations between the two PJ phases. The TCs during the positive PJ phase averagely recurve at a more northeastward location than those during the negative PJ phase (positive PJ phase: 29.6°N, 136.6°E, negative PJ phase: 27.8°N, 128.7°E) (Table 2). The characteristics can be indicated from results that TC recurvature frequency during the positive PJ phase is higher over the region east of 135°E and that during the negative PJ phase is higher over the mainland China (west of 120°E). The characteristics is also observed in the difference between the two PJ phases that are selected from neutral ENSO years: 73 (about 54%) of the 133 TCs

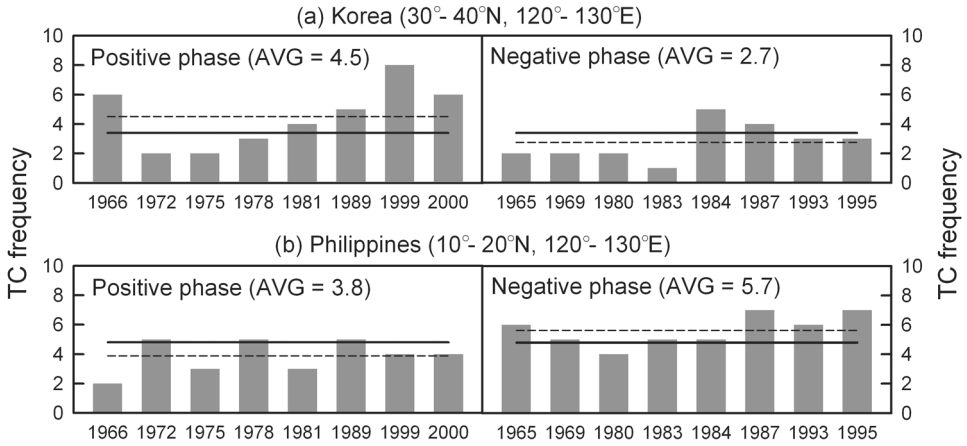

Figure 5. Same as in Figure 3 but for JAS TCPF. Thick solid line is a climatological mean TCPF in each area (Korea: 3.4, the Philippines: 4.8).

recurved during the positive PJ phase and 50 (about 47%) of the 106 TCs during the negative PJ pattern. In addition, TCs during the positive PJ phase averagely recurve at a more northeastward location than those during the negative PJ phase (positive PJ phase: 30.1°N, 136.4°E, negative PJ phase: 27.3°N, 130.7°E) (Table 2). Eventually, the difference in a TC recurvature between the two PJ phases can be related to the TC genesis location and TC track as analyzed above.

[25] On the other hand, the TC central pressure at recurvature is examined in both PJ phases (insets in Figure 6). For two PJ phases including and excluding ENSO years, it can be indicated that the TC mean central pressure at recurvature during the positive PJ phase is deeper than during the negative PJ phase, which implies that TC intensity is stronger during the positive PJ phase (Table 2). This may be because more TCs during the negative PJ phase are affected by the terrain during passing through the mainland China, as can be seen in Figures 4b and 4c. In the following subsection, this difference in the TC intensity between the two PJ phases is examined in detail and its possible cause is explained.

4.4. TC Intensity

[26] In order to investigate whether the difference in the TC track between the two PJ phases has influence on the TC intensity, this study analyzes the TC lifetime and the TC minimum central pressure during the TC life cycle for the two PJ phases. Here, the TC lifetime is defined as the period from the occurrence to the disappearance of a TC in an RSMC best-track data set with 6-h intervals. Also, the TC minimum central pressure is defined as the deepest central pressure recorded for the TC lifetime in the same data.

[27] In the TC lifetime, the climatological mean value of TCs occurred during the boreal summer over the subtropical WNP is approximately 9 days (Figure 7a). However, the TC lifetime during the negative PJ phase with ENSO years is 1 day shorter than the climatological mean value. Furthermore, it shows a greater difference (3.2 days) from that during the positive PJ phase with ENSO years (Table 2).

[28] The difference in the TC minimum central pressure between the two PJ phases with ENSO years shows the similar characteristics to the TC lifetime. The TC minimum central pressure during the negative PJ phase is higher than the climatological mean value, which, in particular, shows a difference of about 10 hPa from that during the positive PJ pattern (Table 2). This result is nearly same as the difference in the TC central pressure at recurvature between the two PJ phases with ENSO years. This feature in TC intensity is also shown in the difference between the two PJ phases that are selected from neutral ENSO years (Figure 7b), although its difference is not as large as that between the two PJ phases with ENSO years. However, the difference in averages between the two PJ phases for TC intensity (both TC lifetime and TC minimum central pressure) is significant at the 99% confidence level (Table 2).

[29] As a result of our detailed investigation, the reason why TCs during the negative PJ phase are weaker in intensity is analyzed as follows: (i) TCs move westward and then get dissipated as soon as they make landfall in southern China. (ii) TCs make landfall in southern China and then dissipate during their passage through the mainland China due to the terrain effect. However, TCs during the positive PJ phase can spend a long time acquiring abundant energy from the ocean, allowing them to develop significantly while moving northward toward the midlatitudes of East Asia, as shown in Figures 4b and 4c.

[30] In the following sections, factors leading to the difference in the TC activity between the two PJ phases are diagnosed through the analyses of the large-scale atmospheric circulation and the SST.

4.5. Large-Scale Atmospheric Environments

[31] Figure 8 shows differences in the zonal vertical wind shear (hereafter, ZVWS) between 200 hPa and 850 hPa levels, streamline at the 850 hPa, and OLR between the positive and the negative PJ phases. In the difference between the two PJ phases with ENSO years, the negative ZVWS is distinctively located along the latitude band of 30°–40°N (Figure 8a). The weak ZVWS indicates the formation of a favorable vertical atmospheric environment for TC genesis and TC development. The negative ZVWS is also predominant between 15°–30°N to the west of 150°E. This region is somewhat consistent with the main region

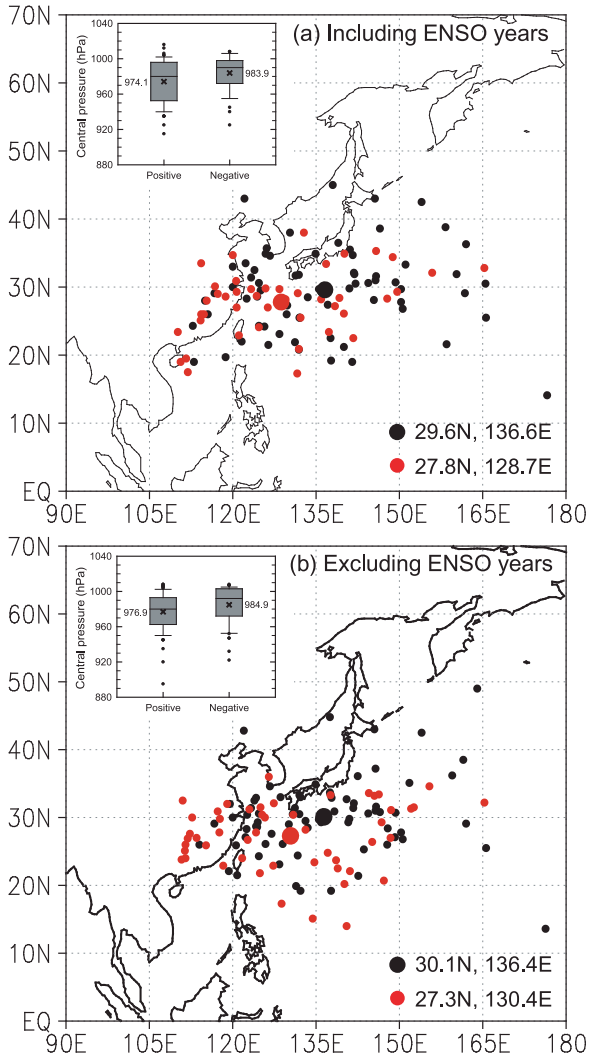

Figure 6. TC recurvature locations for two PJ phases: (a) with ENSO years and (b) selected from neutral ENSO years for JAS. Black and red dots denote TC recurvature locations during the positive and negative PJ phases, respectively. Big dots are the mean recurvature locations. Black and red dot numbers denote mean recurvature locations for the two phases, respectively. The insets show box plots of the TC central pressure at recurvature on two PJ phases. Boxes denote the 25th and 75th percentiles, with the lines in the boxes marking the median and the circles the values below (above) the 25th (75th) percentiles of the distributions. Numbers inside the insets represent averages (cross marks) in each phase.

(blue circles) of a TC genesis during the positive PJ phase. In addition, the region of the negative ZVWS over the WNP to the south of 40°N generally matches the main region of a TCPF (red circles) during the positive PJ phase. This environment of a ZVWS during the positive PJ phase can be one factor contributing to the strengthening of TC intensity.

[32] In the 850 hPa streamline, there are two huge anomalous circulations over the WNP (Figure 8b); the cyclonic circulation centered to the northeast of Taiwan, and the anticyclonic circulation centered to the east of Japan. The Korea, which is located between these two huge circulations, is affected by southeasterly. This southeasterly acts as steering flow that pushes TCs to move northward from the northeast of the Philippines, passing through the East China Sea, to Korea and Japan, as indicated in Figure 4b. Therefore, the TCPF around Korea is higher during the positive PJ phase by this southeasterly derived from the two huge circulations. In addition, TCs move over the ocean along these steering flows and thus can have a long time acquiring abundant energy from the ocean, allowing them to develop quickly while moving northward toward the midlatitudes of East Asia, as stated above. This can be an important reason why TCs during the positive PJ phase are much stronger in the intensity than those during the negative PJ phase which move westward and then get dissipated as soon as they make landfall in the southern China, or make landfall in southern China and dissipate during their passage through the mainland China due to the terrain effect. However, westerly over the Southeast Asian region (e.g., the Philippines, South China Sea, and southern China) prevents TCs from moving westward toward this region during the positive PJ phase. These large-scale features at the 850 hPa level during the positive PJ phase are also observed at the 500 hPa level (not shown).

[33] On the other hand, the cyclonic circulation centered to the northeast of Taiwan develops northward near 30°N. This implies that a WNPH during the positive PJ phase develops more northward than that during the negative PJ phase. This result is distinctively indicated by 5870 gpm contours that can be defined as a boundary line of a WNPH for the two PJ phases, as shown in Figures 4b and 4c. The WNPH during the positive PJ phase is located more toward the north than that during the negative PJ phase. Instead, a WNPH during the negative PJ phase extends westward toward southern China. Generally, TC tends to move northward around the southwestern periphery of the WNPH. *Tu et al.* [2009] demonstrated the main track of a TC also shifts toward Taiwan and the East China Sea since 2000 due to the northward displacement of a WNPH. In the present study also, main tracks of TCs during the two PJ phases agree well with the western periphery of a WNPH in both PJ phases. In addition, the monsoon trough of a huge cyclonic circulation extends eastward from southern China to near 165°E (Figure 8b). This result implies that convection over the subtropical WNP is more active during the positive PJ phase, which can be one evidence that TCs during this PJ phase occur more than during the negative PJ phase.

[34] This feature related to the difference in a convective activity over the subtropical WNP between the two PJ phases also can be shown through OLR analysis (Figure 8c). Here, as described above, since OLR data is available from 1974 (except for the year 1978), data in PJ years including this period is used in OLR analysis. The negative OLR is predominant between 10°–30°N during the positive phase. In particular, its center is located in the region of 15°–25°N, which is generally consistent with the main region of a TC genesis during the positive PJ phase, as analyzed in Figure 2b. Moreover, the strengthened convective activity over the subtropical WNP can be indicated through the analysis of the composite difference of a latitude-pressure cross-section of the vertical velocity and the meridional circulation averaged along 120°–160°E between the two PJ phases (Figure 9). Here, the longitude band of 120°–160°E is defined as the main region of a TC genesis during the two PJ phases in

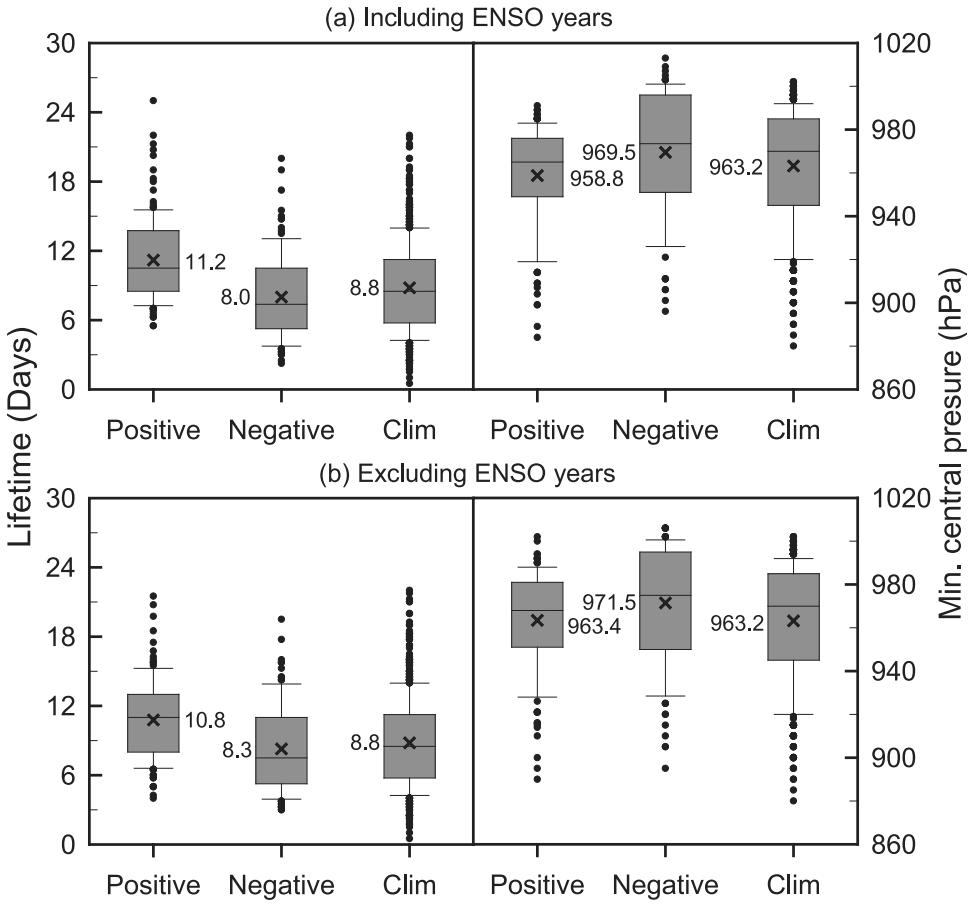

Figure 7. Same as insets in Figure 6 but for (left) TC lifetime and (right) minimum central pressure during the entire TC lifetime for two PJ phases: (a) with ENSO years and (b) selected from neutral ENSO years for JAS. "Clim" represents climatology for 1965–2008.

Figure 2b. The upward flows over the region between 15°–30°N are also strengthened through all levels during the positive PJ phase, with the result that their center is located in the latitude band of 20°–25°N.

[35] The characteristics in the large-scale atmospheric environments between the two PJ phases with ENSO years is clearly demonstrated in those between the two PJ phases that are selected from neutral ENSO years as well (right in Figure 8).

4.6. SST Environment

[36] The role of SST also cannot be overlooked in the TC genesis and TC development. Therefore, this study analyzes the difference in the SST between the two PJ phases (Figure 10). In the difference between the two PJ phases with ENSO years (Figure 10a), the result shows a spatial distribution similar to La Niña pattern. This is because there is a weak negative relationship between the PJ pattern and ENSO, as analyzed above. In general, convection in La Niña years shifts toward the region northwest of the subtropical WNP and thus more TCs tends to occur over this region [*Wang and Chan*, 2002; *Elsner and Liu*, 2003; *Chen et al.*, 2006]. This is well consistent with a result that more TCs during the positive PJ phase tend to occur in the region northwest of the subtropical WNP. The effect of ENSO on a WNP TC activity has already been investigated by a number of studies [*Chan*, 1985; *Dong*, 1988; *Lander*, 1994; *Chan*, 2000; *Wang and Chan*, 2002; *Chu*, 2002, 2004; *Wu et al.*, 2004; *Camargo and Sobel*, 2005; *Camargo et al.*, 2007].

[37] On the other hand, the difference between the two PJ phases that are selected from neutral ENSO years also shows a similar spatial distribution to the difference between the two PJ phases with ENSO years, but it is similar to much weaker La Niña pattern. Therefore, the changes of the TC activity by the PJ pattern analyzed above can be characterized in non-ENSO years as well as ENSO years. Another important thing in the result of a SST analysis is that except for some regions of the subtropical WNP, most regions over the WNP are covered with warm SST. In particular, it is more distinctive in the midlatitudes of East Asia. This condition of SST may provide a favorable environment for the strengthening of TC intensity during the positive PJ phase.

4.7. Comparison With ENSO Pattern

[38] In the above sections, it is shown that the SST spatial distribution similar to La Niña pattern is strengthened during the positive PJ phase. In addition, the PJ pattern shows a weak negative relation with ENSO. These results imply that the positive (negative) PJ phase can correspond to the La Niña (El Niño) phase, although the characteristics in difference between the two PJ phases that are selected from

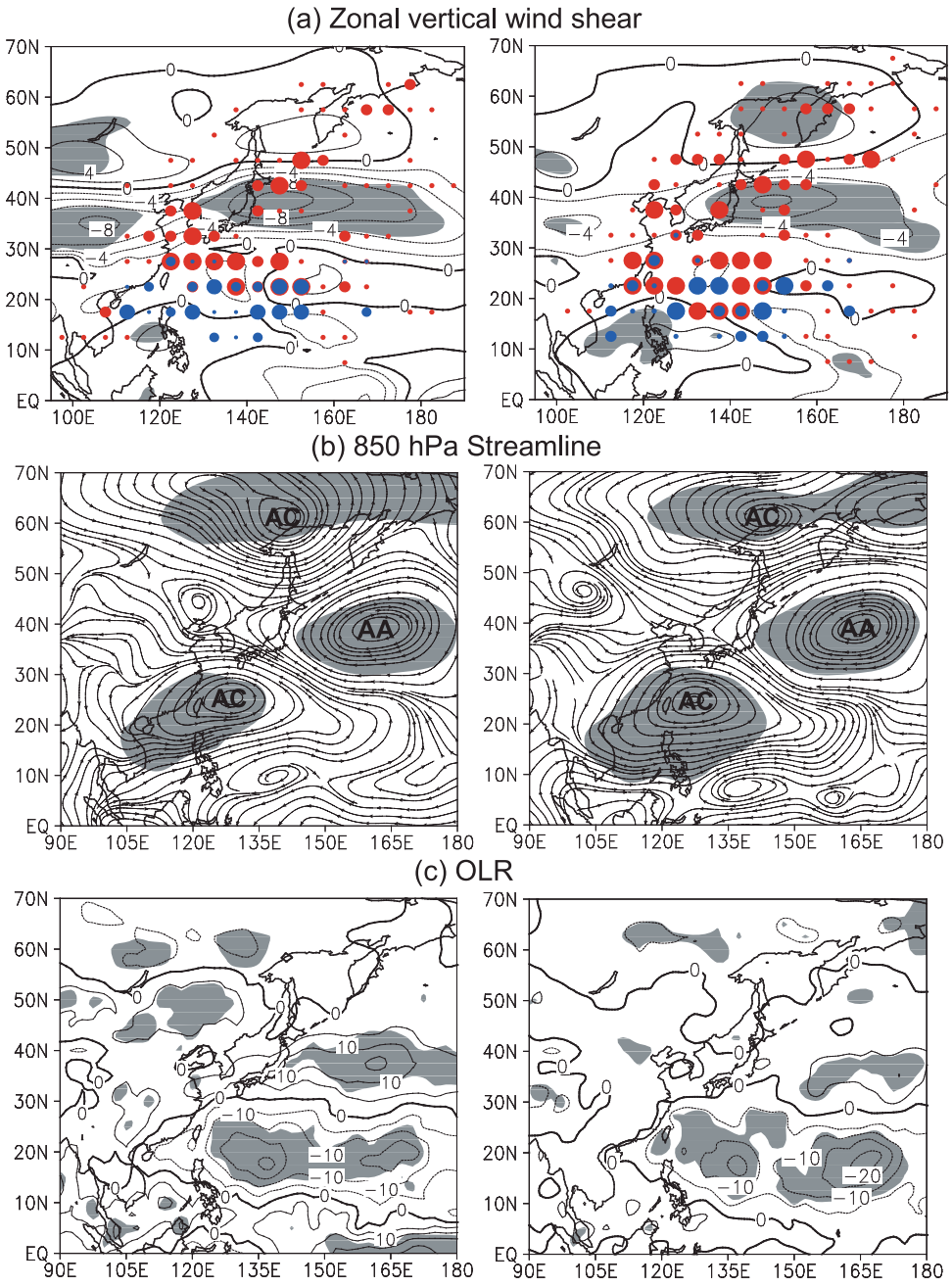

Figure 8. Differences in (a) zonal vertical wind shear (ZVWS, 200–850 hPa), (b) 850 hPa streamline, and (c) OLR between positive and negative PJ phases (left) with ENSO years and (right) selected from neural ENSO years for JAS. Shaded areas denote regions with confidence level higher than 95%. In Figure 8a, red and blue circles represent regions where TCGF and TCPF are distinctive during the positive PJ phase respectively, and their legends are the same as in Figures 2b and 4b. Contour intervals are 2 m s^{-1} for ZVWS and 5 W m^{-2} for OLR. In Figure 8b, "AA" and "AC" represent anomalous anticyclone and anomalous cyclone, respectively.

neutral ENSO years are similar to those between the two PJ phases with ENSO years. Here, a question can be raised that differences between the two PJ phases might be similar to those between the two ENSO phases, if the PJ pattern is affected by ENSO. Therefore, to compare the characteristics on differences between the two PJ phases and between the two ENSO phases, this study analyzes differences in TC activity and its relation with large-scale atmospheric environments between the average in La Niña years (1970–71, 1973–75, 1985, 1988, 1998–99) and the average for El Niño years (1965, 1972, 1982, 1986–97, 1991, 1994, 1997, 2002, 2004, 2006) (Figure 11). Here, since OLR data is available from 1974 (except for the year 1978), data in years of two ENSO phases including this period is used in this analysis.

[39] Average TCGFs in 9 La Niña years and 11 El Niño years are 14.3 (129 TCs) and 15.2 (167 TCs) respectively,

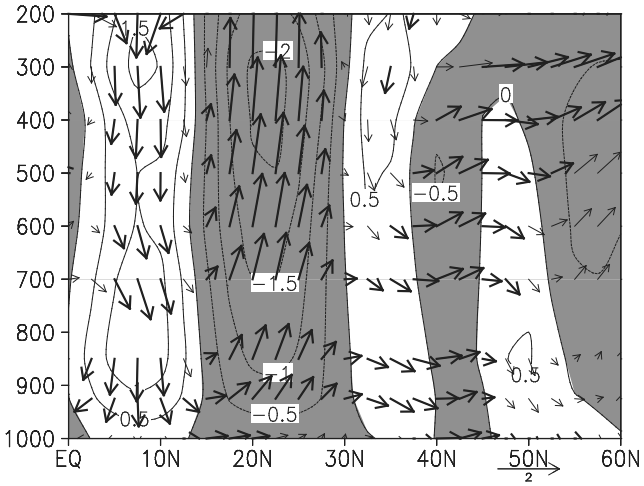

Figure 9. Composite difference in latitude-pressure cross-section of vertical velocity (contour) and meridional circulation (vector) averaged along 120°–160°E between the positive and the negative PJ phases with ENSO years for JAS. The values of vertical velocity are multiplied by −100. Shaded areas indicate negative vertical velocity. Thick arrows are significant at the 95% confidence level. Contour interval is 0.5^{-2} hPa s^{-1}.

and TCs during the La Niña phase averagely are located more toward the northwest (La Niña phase: 18.3°N, 140.1°E, El Niño phase: 14.8°N, 144.5°E). Between the two ENSO phases, the difference in the TCGF is not statistically significant, but differences in the latitude and longitude of TC genesis location are significant at the 99% confidence level. These results are similar to the feature of the difference in the TC genesis location between the two PJ phases, but opposite to that in the TCGF. The difference in TCGF in each 5° × 5° grid box between the two ENSO phases shows the spatial distribution similar to that between the two PJ phases (blue circles in Figure 11a). However, the difference in TCPF between the two ENSO phases is somewhat different from that between the two PJ phases. While in the difference between the two PJ phases, the dipole-like pattern between the regions of Southeast and Northeast Asia is distinctive over the WNP (Figures 4a and 4b), TCs during the La Niña phase tend to migrate northward along the East Asian coast from Philippines, passing through East China Sea, to Korea and Japan. These differences in TC activity between the two ENSO phases dose not appear to mach with the spatial distribution of the difference in the ZVWS between the two ENSO phases (Figure 11a). While the negative ZVWS that is strengthened between 30°–40°N is similar to that between the two PJ phases, the spatial distribution in the region south of 30°N is nearly opposite to that between the two PJ phases. However, the frequent passage of TC along the East Asian coast during the La Niña phase can be explained from the result of the difference in the 850 hPa streamline between the two ENSO phases (Figure 11b). While in the difference between the two PJ phases, two huge anomalous circulations are located over the WNP (Figure 8b), only one huge anticyclonic circulation exits over the WNP in the difference between the two ENSO phases. Southerly derived from this anticyclonic circulation is predominant over the regions along the East Asian coast, which likely acts as steering flow that pushes TCs to move northward toward the same regions. On the other hand, the difference in OLR between the two ENSO phases is similar to that between the two PJ phases (Figure 11c). In other words, south-high and north-low pattern is distinctive in the region south of 30°N, although the negative OLR region between 20°–30°N is meridionally narrow comparing to that between the two PJ phases. As a result, TCs during the La Niña phase have a tendency to occur more toward the northwest than those during the El Niño phase, as analyzed in the difference between the two PJ phases.

[40] Overall, from the above analysis, it is not clear whether the characteristics of TC activity and its relation with the large-scale atmospheric environments by the PJ pattern are directly affected by ENSO or not.

5. Concluding Remarks

[41] This study has examined changes of WNP TC activity by the PJ pattern that is one of the main summer atmospheric circulation patterns in East Asia. The highest 8 PJ years and the lowest 8 PJ years with and without ENSO years are defined, respectively. In the difference between the positive and negative PJ phases with ENSO years, two huge

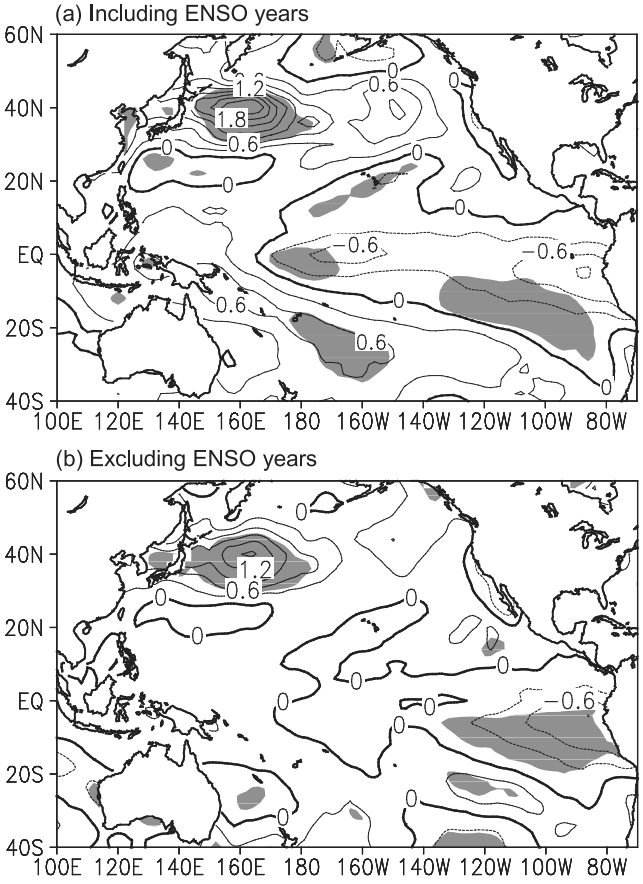

Figure 10. Composite difference in SST between positive and negative PJ phases (a) with ENSO years and (b) selected from neural ENSO years for JAS. Shaded areas denote regions with confidence level greater than 95%. Contour interval is 0.3°C.

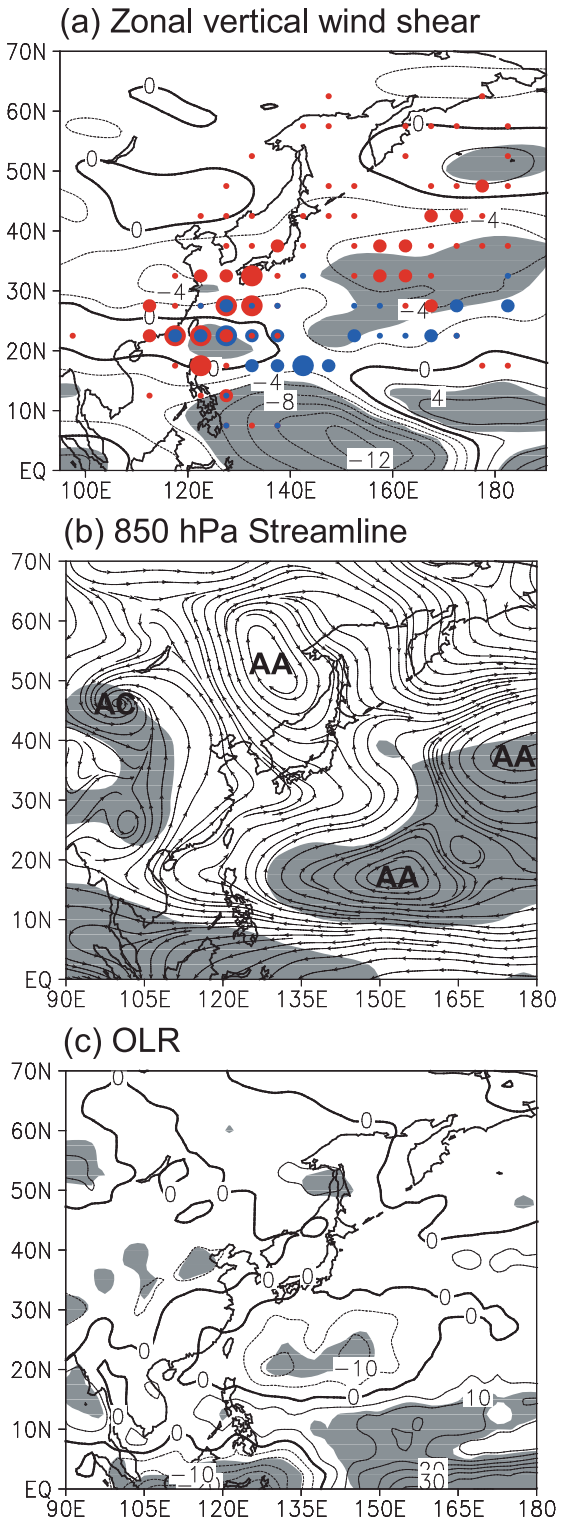

Figure 11. Same as in Figure 8 but for differences between averages for La Niña and El Niño years. Shaded areas denote regions with confidence level higher than 95%. In Figure 11a, red and blue circles represent regions where TCGF and TCPF are distinctive during the La Niña years respectively, and their legends are the same as in Figures 2b and 4b. Contour intervals are 2 m s^{-1} for ZVWS and 5 W m^{-2} for OLR. In Figure 11b, "AA" and "AC" represent anomalous anticyclone and anomalous cyclone, respectively.

circulations in East Asia are strengthened during the positive PJ phase: (i) cyclonic circulation that extends eastward from the east of Taiwan to the east of the subtropical WNP, and (ii) anticyclonic circulation located in the midlatitudes of East Asia (centered to the east of Japan). The cyclonic circulation in the subtropical WNP indicates that convective activity is strengthened in this region during the positive PJ pattern, which is also observed through the analysis of differences between the two PJ phases on OLR and meridional circulation over the WNP. As a result, more TCs occur during this PJ phase. In particular, as convective center is located between 15°–25°N in the WNP, TCs during the positive PJ phase tend to occur in the region north of 15°N. On the other hand, the anticyclonic circulation to the east of Japan acts as steering flow that pushes TCs northward from the northeast of Philippines, passing through the East China Sea, to Korea and Japan. On the contrary, TCs during the negative PJ phase tend to move westward toward the South China Sea and southern China. In other words, as the TC track during the positive PJ phase is more active to the northeast than those during the negative PJ phase and a dipole-like pattern between the regions of Southeast and Northeast Asia is shown in the difference in the TCPF between the two PJ phases. The schematic diagrams on the TC activity that can be strengthened during the positive PJ phase are illustrated in Figure 12 and more detailed statistics on TC activity during the two PJ phases is presented in Table 2.

[42] These differences in the TC genesis and the TC track between both PJ phases also have an effect on TC intensity (TC lifetime and TC minimum central pressure). TCs during the positive PJ phase can spend a long time acquiring abundant energy from the ocean, allowing them to develop significantly while moving northward toward the midlatitudes of East Asia. However, TCs during the negative PJ phase move westward and then get dissipated as soon as they make landfall in southern China, or make landfall in southern China and then dissipate during the passage through the mainland China due to the terrain effect. In addition, the

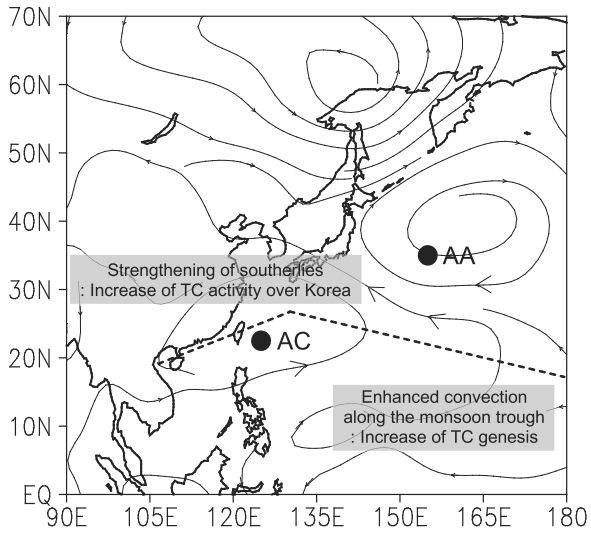

Figure 12. Schematic illustration of atmospheric changes during the positive PJ phase. "AA" and "AC" represent anomalous anticyclone and anomalous cyclone, respectively. The dashed line denotes a monsoon trough.

regions of the high TCGF and high TCPF during the positive PJ phase generally agree with weak ZVWS regions and with the warm SST regions. Eventually, more favorable atmospheric and oceanic environments for the TC genesis and TC intensity are formed during the positive PJ phase.

[43] The characteristics of TC activities that is strengthened during the positive PJ phase with ENSO years is similar to that during the positive PJ phase that are selected from neutral ENSO years. In particular, as the difference in the SST between the positive and negative PJ phases shows the spatial distribution like a La Niña pattern, the difference between La Niña and El Niño phases is analyzed to compare with those between the two PJ phases. As a result, while the feature of a TC genesis location is similar to that between the two PJ phases, a TCPF shows the different pattern. In other words, TCs during the La Niña phase tend to move northward along the East Asian coast from Philippines, passing through the East China sea, to Korea and Japan.

[44] Oh the other hand, analysis results of the relationship between PJ pattern and WNP TC activity are still unsatisfactory, because the priority of the two variables is still not clear, as discussed above. Therefore, in order to effectively examine the relationship between the two variables, additional studies using the numerical model are required in follow-up papers.

[45] **Acknowledgments.** This work is supported by NSC98-2111-M-002-008-MY3. The authors wish to thank two anonymous reviewers for their valuable suggestions and reviews that led to the improvement of this paper.

References

Camargo, S. J., and A. Sobel (2005), Western North Pacific tropical cyclone intensity and ENSO, *J. Clim.*, *18*, 2996–3006, doi:10.1175/JCLI3457.1.

Camargo, S. J., A. W. Robertson, S. J. Gaffney, P. Smyth, and M. Ghil (2007), Cluster analysis of typhoon tracks: Large-scale circulation and ENSO, *J. Clim.*, *20*, 3654–3676, doi:10.1175/JCLI4203.1.

Chan, J. C.-L. (1985), Tropical cyclone activity in the northwest Pacific in relation to the El Niño/Southern Oscillation phenomenon, *Mon. Weather Rev.*, *113*, 599–606, doi:10.1175/1520-0493(1985)113<0599:TCAITN>2.0.CO;2.

Chan, J. C.-L. (2000), Tropical cyclone activity over the western North Pacific associated with El Niño and La Niña events, *J. Clim.*, *13*, 2960–2972, doi:10.1175/1520-0442(2000)013<2960:TCAOTW>2.0.CO;2.

Chen, T.-C., S.-Y. Wang, and M.-C. Yen (2006), Interannual variation of the tropical cyclone activity over the western North Pacific, *J. Clim.*, *19*, 5709–5720, doi:10.1175/JCLI3934.1.

Chia, H.-H., and C. F. Ropelewski (2002), The interannual variability in the genesis location of tropical cyclones in the northwest Pacific, *J. Clim.*, *15*, 2934–2944, doi:10.1175/1520-0442(2002)015<2934:TIVITG>2.0.CO;2.

Choi, K.-S., and H.-R. Byun (2010), Possible relationship between western North Pacific tropical cyclone activity and Arctic Oscillation, *Theor. Appl. Climatol.*, *100*, 261-274, doi:10.1007/s00704-009-0187-9.

Chu, P.-S. (2002), Large-scale circulation features associated with decadal variations of tropical cyclone activity over the central North Pacific, *J. Clim.*, *15*, 2678–2689, doi:10.1175/1520-0442(2002)015<2678:LSCFAW>2.0.CO;2.

Chu, P.-S. (2004), ENSO and tropical cyclone activity, in *Hurricanes and Typhoons: Past, Present, and Potential*, edited by R. J. Murnane and K.-B. Liu, pp. 297–332, Cambridge Univ. Press, Cambridge, U. K.

Dong, K. (1988), El Niño and tropical cyclone frequency in the Australian region and the northwest Pacific, *Aust. Meteorol. Mag.*, *36*, 219–225.

Elsner, J. B., and K. B. Liu (2003), Examining the ENSO-typhoon hypothesis, *Clim. Res.*, *25*, 43–54, doi:10.3354/cr025043.

Ho, C.-H., J.-H. Kim, H.-S. Kim, C.-H. Sui, and D.-Y. Gong (2005), Possible influence of the Antarctic Oscillation on tropical cyclone activity in the western North Pacific, *J. Geophys. Res.*, *110*, D19104, doi:10.1029/2005JD005766.

Huang, R.-H., and W.-J. Li (1987), Influence of the heat source anomaly over the western tropical Pacific on the subtropical high over East Asia, paper presented at International Conference on the General Circulation of East Asia, ICGCEA, Chengdu, China.

Kalnay, E., et al. (1996), The NCEP/NCAR 40-Year Reanalysis Project, *Bull. Am. Meteorol. Soc.*, *77*, 437–471, doi:10.1175/1520-0477(1996)077<0437:TNYRP>2.0.CO;2.

Kawamura, R., and T. Ogasawara (2006), On the role of typhoons in generating PJ teleconnection patterns over the western North Pacific in late summer, *SOLA*, *2*, 37–40, doi:10.2151/sola.2006-010.

Kawamura, R., T. Murakami, and B. Wang (1996), Tropical and midlatitude 45-day perturbations over the western Pacific during the northern summer, *J. Meteorol. Soc. Jpn.*, *74*, 867–890.

Kawamura, R., M. Sugi, T. Kayahara, and N. Sato (1998), Recent extraordinary cool and hot summers in East Asia simulated by an ensemble climate experiment, *J. Meteorol. Soc. Jpn.*, *76*, 597–617.

Kistler, R., et al. (2001), The NCEP/NCAR 50-year reanalysis, *Bull. Am. Meteorol. Soc.*, *82*, 247–267, doi:10.1175/1520-0477(2001)082<0247:TNNYRM>2.3.CO;2.

Kosaka, Y., and H. Nakamura (2006), Structure and dynamics of the summertime Pacific-Japan teleconnection pattern, *Q. J. R. Meteorol. Soc.*, *132*, 2009–2030, doi:10.1256/qj.05.204.

Kurihara, K., and T. Tsuyuki (1987), Development of the barotropic high around Japan and its association with Rossby wave–like propagations over the North Pacific: Analysis of August 1984, *J. Meteorol. Soc. Jpn.*, *65*, 237–246.

Lander, M. A. (1994), An exploratory analysis of the relationship between tropical storm formation in the western North Pacific and ENSO, *Mon. Weather Rev.*, *122*, 636–651, doi:10.1175/1520-0493(1994)122<0636:AEAOTR>2.0.CO;2.

Liebmann, B., and C. A. Smith (1996), Description of a complete (interpolated) outgoing longwave radiation dataset, *Bull. Am. Meteorol. Soc.*, *77*, 1275–1277.

McBride, J. L. (1995), Tropical cyclone formation, in *Global Perspective on Tropical Cyclones*, *WMO/TD 693*, pp. 63–105, World Meteorol. Org., Geneva.

Murakami, T., and J. Matsumoto (1994), Summer monsoon over the Asian continent and the western North Pacific, *J. Meteorol. Soc. Jpn.*, *72*, 719–745.

Nitta, T. (1986), Long-term variations of cloud amount in the western Pacific region, *J. Meteorol. Soc. Jpn.*, *64*, 373–390.

Nitta, T. (1987), Convective activities in the tropical western Pacific and their impact on the Northern Hemisphere summer circulation, *J. Meteorol. Soc. Jpn.*, *65*, 373–390.

Nitta, T. (1989), Global features of the Pacific-Japan oscillation, *Meteorol. Atmos. Phys.*, *41*, 5–12, doi:10.1007/BF01032585.

Reynolds, R. W., N. A. Rayner, T. M. Smith, D. C. Stokes, and W. Wang (2002), An improved in situ and satellite SST analysis for climate, *J. Clim.*, *15*, 1609–1625, doi:10.1175/1520-0442(2002)015<1609:AIISAS>2.0.CO;2.

Tsuyuki, T., and K. Kurihara (1989), Impact of convective activity in the western tropical Pacific on the East Asian summer circulation, *J. Meteorol. Soc. Jpn.*, *67*, 231–247.

Tu, J.-Y., C. Chou, and P.-S. Chu (2009), The abrupt shift of typhoon activity in the vicinity of Taiwan and its association with western North Pacific−East Asian climate change, *J. Clim.*, *22*, 3617–3628, doi:10.1175/2009JCLI2411.1.

Wakabayashi, S., and R. Kawamura (2004), Extraction of major teleconnection patterns possibly associated with the anomalous summer climate in Japan, *J. Meteorol. Soc. Jpn.*, *82*, 1577–1588, doi:10.2151/jmsj.82.1577.

Wang, B., and J. C.-L. Chan (2002), How strong ENSO events affect tropical storm activity over the western North Pacific, *J. Clim.*, *15*, 1643–1658, doi:10.1175/1520-0442(2002)015<1643:HSEEAT>2.0.CO;2.

Wilks, D. S. (1995), *Statistical Methods in the Atmospheric Sciences*, 467 pp., Academic, San Diego, Calif.

Wu, M.-C., W.-L. Chang, and W.-M. Leung (2004), Impacts of El Niño–Southern Oscillation events on tropical cyclone landfalling activity in the western North Pacific, *J. Clim.*, *17*, 1419–1422.

Yamada, K., and R. Kawamura (2007), Dynamical link between typhoon activity and the PJ teleconnection pattern from early summer to autumn as revealed by the JRA-25 Reanalysis, *SOLA*, *3*, 65–68, doi:10.2151/sola.2007-017.

E.-J. Cha, National Typhoon Center, Korea Meteorological Administration, Jeju 699-942, South Korea. (kenkyukan@korea.kr)

K.-S. Choi and C.-C. Wu (corresponding author), Department of Atmospheric Sciences, National Taiwan University, Taipei 106, Taiwan. (cwuchoi@typhoon.as.ntu.edu.tw; cwu@typhoon.as.ntu.edu.tw)